Chemical Engineering Journal 156 (2010) 571–577

Contents lists available at ScienceDirect

Chemical Engineering Journal

journal homepage: www.elsevier.com/locate/cej

Photocatalytic membrane reactor for degradation of acid red B wastewater☆

Huabing Jiang[a], Guoliang Zhang[a,*], Tao Huang[a], Jinyuan Chen[a], Qidong Wang[b], Qin Meng[c]

[a] College of Biological and Environmental Engineering, Zhejiang University of Technology, Hangzhou 310014, PR China
[b] Department of Environmental Science and Engineering, Tsinghua University, Beijing 100084, PR China
[c] College of Material & Chemical Engineering, Zhejiang University, Hangzhou 310027, PR China

ARTICLE INFO

Article history:
Received 15 October 2008
Received in revised form 24 March 2009
Accepted 2 April 2009

Keywords:
Acid red B
Titanium dioxide
Photocatalysis
Membrane
Reactor

ABSTRACT

Nano-titanium dioxide (TiO_2) photocatalyst was prepared by acid–sol method using tetrabutyl titanate and ethanol, which appeared to be anatase by XRD analysis. The wastewater containing azo dye acid red B was then subjected to photocatalytic degradation with photocatalyst TiO_2 and UV as light source in a slurry photocatalytic membrane reactor, which included a double layer cylindrical photocatalytic reaction zone and a plate frame membrane separation part. Two kinds of ultrafiltration (UF) membranes PVDF700 and PAN700 were applied and the combined process with photocatalysis was operated by a continuous re-circulating mode during treatment. At first, the adsorption characteristic of the titanium dioxide catalyst under different pH values was analyzed and the optimal operation condition of the photocatalytic process was achieved by changing TiO_2 dose and initial concentration of the dye. Then the performance of photocatalyst separation process by ultrafiltration (UF) was investigated. It was found that the degradation of acid red B was followed by first-order kinetics and the efficiency of photocatalysis can be evaluated by the initial reaction rate. Finally, the conglomeration and hydrophilizion phenomena by TiO_2 in the coupling system and its effect to different ultrafiltration membranes were analyzed.

1. Introduction

More than 10,000 species of dyes and pigments are utilized every year, and over 50% of these dyes are azo dyes which contain one or more azo bonds (–N=N–) and aromatics [1]. The release of wastewater containing these dyes is a dramatic source of aesthetic pollution, eutrophication and perturbations to the environment and aquatic life. Due to the complex molecule structure of azo dyes, conventional methods for waste treatment [2–4] are having several drawbacks and not effective for complete degradation of azo dye. Most of these technologies including chemical or biological ways [5] can only break little part of the azo bonds and remove some degree of color, while the azo linkages are just reduced to aromatic amines that are colorless but can also be toxic and potentially carcinogenic. Therefore, it is urgent to develop novel technology of water purification leading to complete destruction of the dangerous azo dyes.

The advanced oxidation processes (AOPs) [6] have been proposed as the alternative methods for organic wastewater purification in recent years. AOPs are efficient novel methods useful to accelerate the non-selective oxidation and thus the destruction of a wide range of organic substances resistant to conventional technology. Among AOP technologies, photocatalytic technology has demonstrated to be very effective to degrade different azo dyes. The photocatalysts usually are some metal oxides such as TiO_2, ZnO, $SrTiO_3$, and $CdS{\cdot}TiO_2$. Photocatalytic oxidization appears as the most potential technology because of its largely available, inexpensive, non-toxic, relatively high chemical stability. The key advantage [7–9] of this method is based on its destructive nature: it does not involve mass transfer, can be carried out under ambient conditions (atmospheric oxygen) and may lead to complete mineralization of azo dyes into CO_2, H_2O and inorganic anions.

According to literatures, there are two forms of titanium dioxide: suspended and immobilized. Taking account of photocatalytic efficiency, the suspended TiO_2 holds some advantageous compared with the immobilized as to its fast mass transfer and larger reaction areas in the same quantity [10,11]. But suspended photocatalytic system has been held back exactly by the problem of catalyst conservation and water/catalyst separation in which the discharging TiO_2 with effluent might do harm to human life due to its biological accumulative effect [12]. To solve these problems, the combining system-photocatalytic membrane reactor has been adopted. Novel photocatalytic membrane reactor utilizes the competitive separation characteristic of membrane compared with conventional separation technologies to continuously separate and maintain high quality of TiO_2 constant in photocatalytic reactor, in the meantime, the coupling effect will turn up to increase anti-contaminated property of membrane [13,14].

☆ This paper was presented at the 12th Asia Pacific Confederation of Chemical Engineers (APCChE08), at Dalian, P.R. China, 4–6 August 2008.

* Corresponding author. Tel.: +86 571 88320863; fax: +86 571 88320863.
E-mail address: guoliangz@zjut.edu.cn (G. Zhang).

1385-8947/$ – see front matter © 2009 Elsevier B.V. All rights reserved.
doi:10.1016/j.cej.2009.04.011

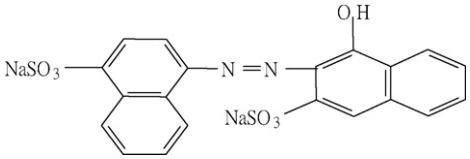

Fig. 1. Structure of acid red B.

The objective of this work was to investigate the degradation behavior of simulated wastewater containing acid red B by a slurry photocatalytic membrane reactor, which was performed with suspended TiO_2 and ultrafiltration (UF) membranes under different operating conditions, such as the value of pH, initial dye concentration, dose of TiO_2 and operating time. The effects of operating condition on separation characteristics were studied in detail to establish the optimal state.

2. Experimental

2.1. Materials and reagent

Acid red B was adopted in this experiment as a model pollutant, which was a typical azo dye in the textile industries and was supplied by Zhejiang Runtu Co., China. The chemical structure of the acid red B was shown in Fig. 1. The chromophore was azo bonds (–N=N–) and auxochrome was sulfonic acid group ($-HSO_3$). The dye was negatively charged by dissolving in de-ionized water.

The catalyst used was titanium dioxide prepared by the acid–sol method. At first, 15 mL tetrabutyl titanate was added into anhydrous ethanol. After 20 min intensively stirring, a yellow solution was obtained. Then 30 mL 1 M HNO_3 was added into the solution and stirred tempestuously for 1.5 h. The solution was adjusted at pH 1.5 and followed by agitation for 1.5 h to give a transparent TiO_2 gel. When the gel was dropped into 35 mL 1 M polyethylene glycol-4000, the pH value was adjusted to 7 and solution was kept stirring 3 h at 100 °C. After that, the gel was washed twice by de-ionized water to deprive of the PEG and dried for 0.5 h at 120 °C. TiO_2 was produced after calcined at 300 °C for 2.5 h. The XRD graph of the titanium dioxide was presented in Fig. 2, which indicated that titanium dioxide was totally anatase. Calculated by Scherrer equation, the average diameter of the crystal was 13.12 nm, and BET of titanium dioxide was 107.44 m^2/g.

Two kinds of self-made ultrafiltration membranes such as PVDF700 and PAN700 were employed in the membrane separation unit. Molecular weight cut-off of both membranes was 70,000 Da and the effective area was 68.56 cm^2 for each disc of modules. According to membrane materials, PVDF was relatively hydrophobic while PAN was hydrophilic. The synthesized wastewater was achieved by dissolving the dyes in de-ionized water. The pH of this synthetic waste effluent was adjusted by the addition of either HCl (10%) or NaOH (10%).

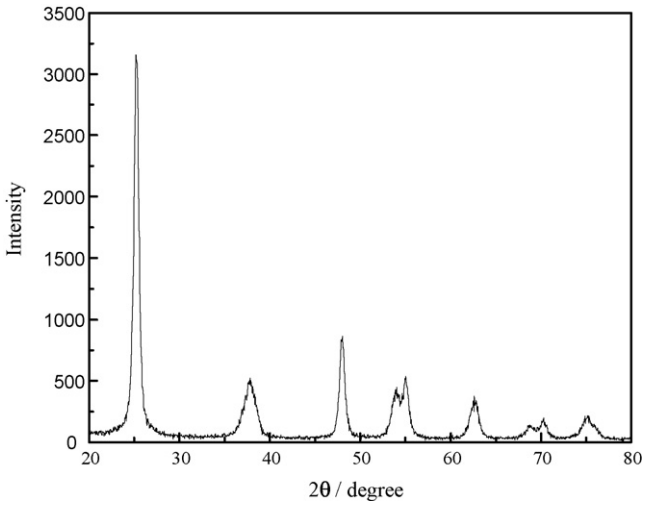

Fig. 2. XRD graph of TiO_2 by acid–sol method.

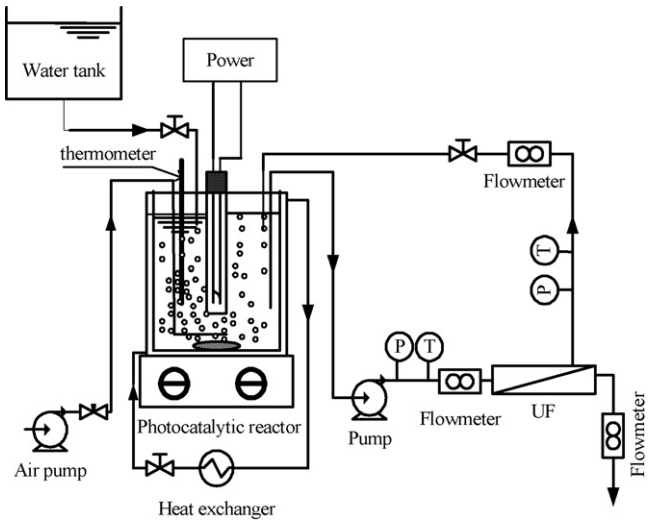

Fig. 3. Schematic diagram of experiment.

2.2. Photocatalytic membrane reactor

Schematic diagram of experiment was shown in Fig. 3, which was composed of a slurry photocatalytic reactor and an ultrafiltration separation unit. The photocatalytic reactor was made of double layer cylindrical Pyrex with an effective volume of 1.2 L, and the outside of the reactor was coated by tinfoil to increase efficiency of UV light. In the center of reactor, a low pressure UV lamp (main wavelength 365 nm, 100 W, Philips YPZ220) equipped with a quartz tube was located and immersed in the dye wastewater. The heat produced by the UV lamp was taken away by the cooling water in the interlayer simultaneously in order to maintain the temperature in reactor at about 20 °C. The magnetic stir at 3000 r/min made titanium dioxide in the dye wastewater suspended. Air was pumped through a gas diffuser placed at the bottom of reactor to ensure small bubble formation for effective purging continuously during treatment.

The photocatalysis treated wastewater containing fine titanium dioxide was transported continuously by a diaphragm pump to membrane separation unit. Velocity of feed was controlled at a range of 0–40 L/h and operating pressure was adjusted by the switches on the retentate pipeline.

2.3. Experimental procedure

Before photocatalytic experiment, the maximal adsorption wavelength (510 nm) of acid red B was determined by a UV–vis spectrophotometer and the calibration curve was got at maximal adsorption wavelength as presented in Fig. 4.

Photocatalytic membrane reaction was performed in three steps. Firstly, the TiO_2 adsorption experiment was tested under different pH values. Then the photocatalytic reaction was established in terms of initial concentration of dye and dose of TiO_2. Through calculation of the initial reaction rate (r_0), the optimum value of both parameters could be obtained. After that, a continuous system coupling photocatalytic oxidation process with ultrafiltration

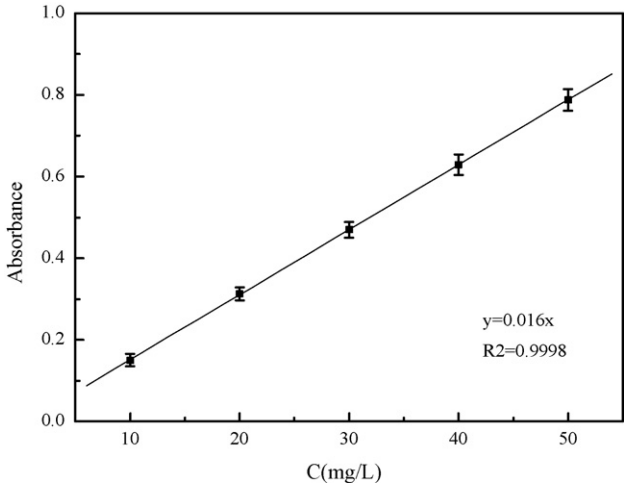

Fig. 4. Calibration curve of acid red B (at 510 nm).

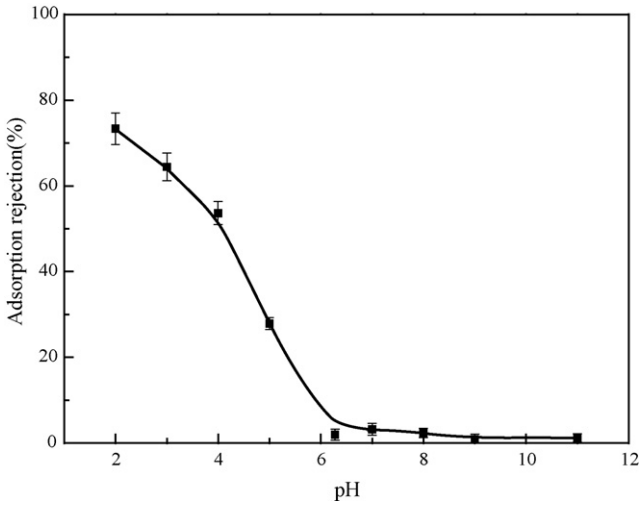

Fig. 5. Effect of pH on TiO_2 adsorption.

was set up. The filtration flux of the membranes and its stabilization was examined.

2.4. Sample analysis

A UV–vis T6 spectrophotometer (Beijing Purkinje General, China) was used for determination of absorbance in range of 200–700 nm. The values of pH and conductivity were measured with a pHs-25 instrument (Rex Analytical, Shanghai, China) and a DDS-11D conductivity detector (Jingke, Shanghai, China). To determine the extent of mineralization of acid red B in waste solution under different conditions, the total organic carbon of reaction solution was measured with a TOC-VCPH total organic carbon analyzer. To figure out the rejection of particular TiO_2, turbidity of the permeate in the process was detected with a SGZ-IP nephelometer (Yuefeng Co., Shanghai, China).

3. Results and discussion

3.1. Effect of pH on adsorption of TiO_2

According to literature [15,16], influence of pH was an important factor during dye adsorption on the photocatalyst. The experiment, with acid red B concentration of 50 mg/L and TiO_2 of 0.5 g/L, was carried out to find optimum value in the range of pH 2–11. The pH was adjusted by adding appropriate amount of NaOH and HCl solution.The result was presented in Fig. 5. It was noted that the highest rejection was achieved in acid solution at pH 2 and decoloration rate was more than 70% after 30 min stirring in dark environment. In neutral and alkaline solution, the removal of color owing to the TiO_2 adsorption was no more than 5%, which indicated that the adsorption contribution to photocatalysis could be neglectable. The possible explanation of these results was the surface charge properties of TiO_2 with pH value around 6.8, which was the point of zero charge (pzc) of TiO_2. It was positively charged in acidic solution (pH < 6.8) and negatively charged in alkaline solution (pH > 6.8). In view of practicality, solution pH of the following tests was set closed to its natural value 6.0 ± 0.2.

3.2. Photocatalytic degradation

To investigate the anti-photolysis of acid red B, the degradation of acid red B in the absence of photocatalyst was performed. Dye concentration of model waste solution was 50 mg/L, and photolysis process was working 120 min under continuously stirring. The rejection rates of color and TOC were shown in Fig. 6. It was observed that decoloration rate increased sharply with the illumination time, while the rejection of TOC rose slowly and mildly. After 120 min irradiation, the rejection of dye and TOC was 82.32% and 23.50%, respectively. The interpretation of this phenomenon was that some of the chromophore was just broken up to smaller molecular organic, leading to the higher rejection of color than TOC. As a result, the simple adsorption or photolysis was not useful to decompose acid red B to innoxious matters, and the intensively photocatalyic degradation reaction was imperative.

3.2.1. Effect of catalyst concentration

During photocatalytic process, one of the most important parameters in operation was dose of catalyst. The effect of different TiO_2 dose on photocatalytic oxidation of acid red B was then carried out. Experimental data demonstrated that the degradation of acid red B obeyed the first order reaction. The observed degradation constant k can be calculated by the following equation [17]:

$$\frac{C_t}{C_0} = e^{-kt} \quad (1)$$

where C_t and C_0 were dye concentrations at t and zero time, respectively.

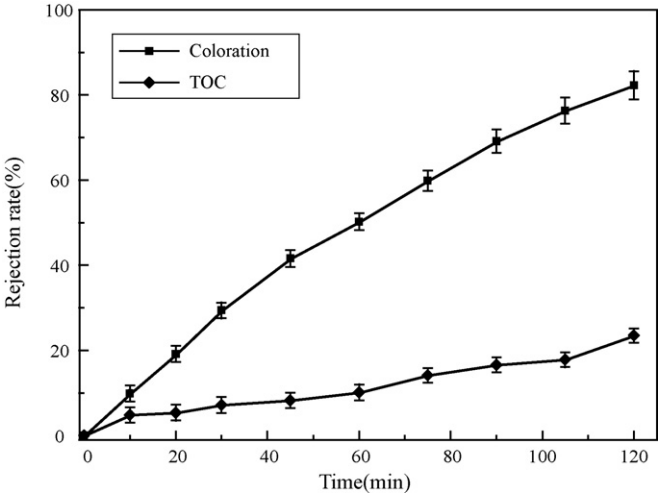

Fig. 6. Photolysis of acid red B without catalyst.

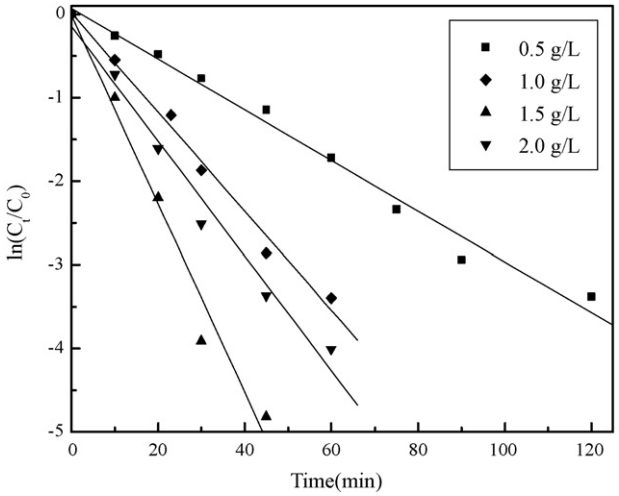

Fig. 7. $\ln(C_t/C_0)$ vs. t.

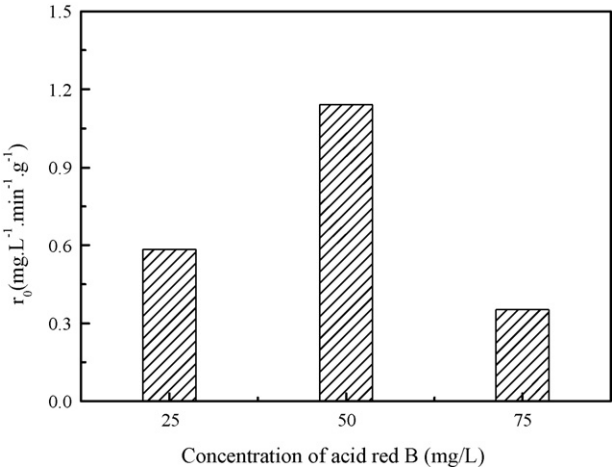

Fig. 8. Effect of initial dye concentration on photocatalysis process.

By plotting $\ln(C_t/C_0)$ vs. t, as presented in Fig. 7, the value of k can be obtained from the reciprocal of the curve slope. The half life time ($t_{1/2}$) could be obtained by the following equation:

$$t_{1/2} = \frac{\ln 2}{k} = \frac{0.693}{k} \quad (2)$$

Due to the photocatalytic process including solid and liquid phases, the degradation efficiency could be denoted by the initial reaction rate (r_0):

$$r_0 = k \times \theta \quad (3)$$

where θ (mg/g L) was the dye adsorbed on the TiO_2 after 30 min stirring.

The data in Table 1 demonstrated that the initial reaction rate was increasing with the increase of catalyst concentration below 1.5 g/L and adverse influence came up when catalyst dose was beyond 1.5 g/L. As can be interpreted, at low TiO_2 level, the increase of catalyst might enlarge the active site for adsorption and degradation of acid red B. Too much of catalysts led to the light scattering of UV light and catalyst agglomeration (particle–particle interactions). Therefore, the optimal concentration of TiO_2 was set at 1.5 g/L.

3.2.2. Effect of initial dye concentration

The effect of initial dye concentration was investigated with optimal catalyst dose of 1.5 g/L. The initial reaction rate (r_0) in the function of different dye concentration was represented in Fig. 8.

It was evident that photocatalytic process was depended on initial acid red B concentration. The optimum concentration was 50 mg/L with an initial reaction rate of 1.141 mg/(L min g). When the initial dye concentration was too low, effective reaction area was not enough and the utilization of photons and catalyst was not enough. When initial dye concentration became too high, photo-generation of holes or •OH radicals on the catalyst surface was reduced since the active sites were covered by dye ions. Another possible explanation was that the penetration of UV light through dye became weaker and efficiency of photo-generation of catalyst was lower.

In sum, the optimal concentration was 1.5 g/L for catalyst and 50 mg/L for dye. To evaluate the mineralization of acid red B, TOC of solution in function of illumination time was presented in Fig. 9. After 120 min illumination, the TOC of solution was 5.14 mg/L and the rejection rate of TOC was up to 70%, which indicated that most of acid red B in solution was mineralized and toxicity of benzene was almost removed.

3.3. UF membrane performance

In order to determine the contribution of ultrafiltration membranes in photocatalytic membrane reactor, separation of acid red B (50 mg/L) by PVDF700 and PAN700 membranes was carried out under 0.12 MPa separately. Fig. 10 showed the permeate flux change with time. The J_t/J_0 value of PAN700 was higher compared to PVDF700, which indicated that PAN700 was better in permeate flux and stabilization. After 120 min, the flux of PAN700 decreased from 352.96 L/(m^2 h) to 238.99 L/(m^2 h), while PVDF700 ranged from 228.90 L/(m^2 h) to 123.88 L/(m^2 h). The decline of permeate flux might be mainly attributed to membrane pollution owing to the adsorption of dye molecules. The difference of the flux between both membranes depended on the difference of membrane mate-

Table 1
Effect of TiO_2 dose on photocatalytic reaction parameters.

TiO_2 (g/L)	r_0 (mg/(L min g))	k (min^{-1})	$t_{1/2}$ (min)	R^2
0.5	0.201	0.030	23.1	0.986
1.0	0.071	0.059	11.7	0.989
1.5	1.141	0.113	6.1	0.977
2	0.609	0.069	10.0	0.982

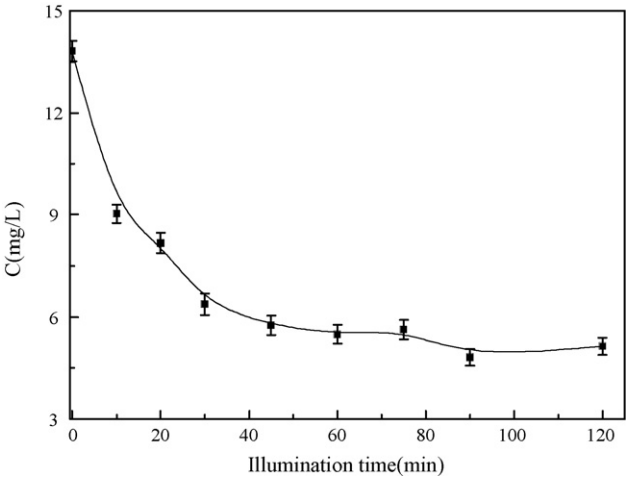

Fig. 9. Mineralization of acid red B in photocatalysis process.

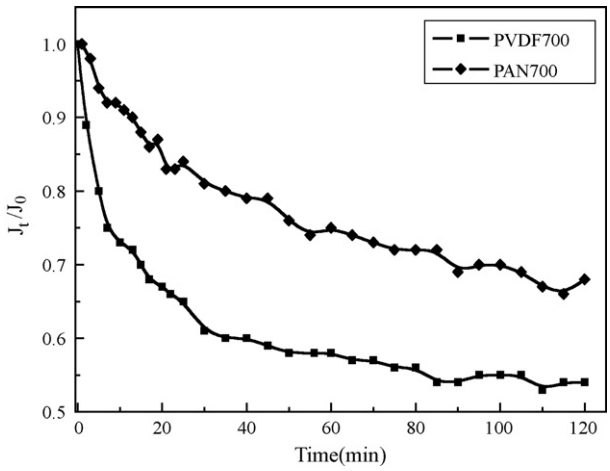

Fig. 10. Separation of azo dye by single membrane unit.

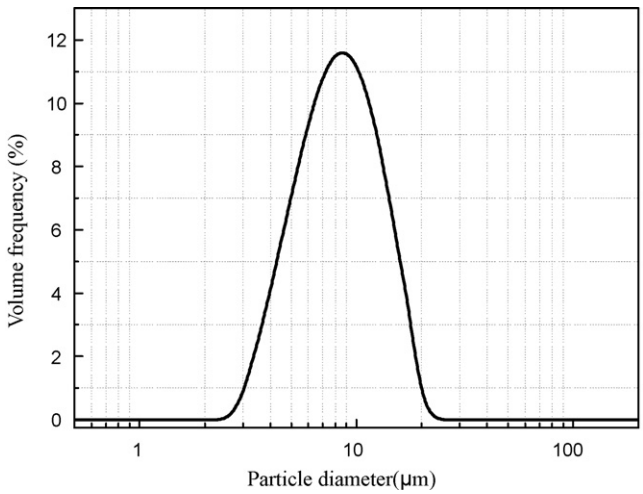

Fig. 12. Size distribution of the TiO_2 particles in solution.

rials. PVDF was more hydrophobic, and in contrast, PAN was more hydrophilic and superior to the water permeability. The rejection of acid red B by both UF membranes could be up to 70%.

3.4. Continuous-recirculation suspended photocatalytic membrane reactor

After the optimal operating conditions for single units were gained, the continuous-recirculation suspended photocatalytic membrane reactor was set up. Acid red B waste solution with volume of 1 L and concentration of 50 mg/L was first stirred in the absence of TiO_2 for 30 min and suspended solution was illuminated 60 min. The UF membrane unit was then coupled with photocatalyst and the feed flux of acid red B solution in water tank was equal to the permeate of UF membrane to keep the volume of solution constant in photocatalytic reactor.

Fig. 11 showed the permeate flux decline with operating time at 0.12 MPa. The curves displayed that the reduction of permeate flux in photocatalytic membrane reactor could be almost neglectable compared with UF separation process. According to low the turbidity of permeate (<0.3 NTU), TiO_2 in photocatalytic treated water was totally retained and recovered. The XRD of catalyst showed that the TiO_2 power particle was 13.12 nm, which indicated that it was hard to retain such particle by the UF membrane theoretically. However, while added into the solution, conglomeration phenomena easily happened between particles [18,19]. As presented in Fig. 12, the average volume diameter was as big as 9.502 μm, which was easily rejected by UF membranes.

The contribution of ultraviolet, photocatalysis and membrane separation with PVDF700 in photocatalytic membrane reactor was shown in Fig. 13. It indicated that the photocatalysis was the most important part in photocatalytic membrane reactor. The fluctuation of decoloration rate with time might be partly attributed to the instability of pilot installation.

The membrane after operation was washed by de-ionized water flush in the disc and TiO_2 cake was easily washed away. The SEM of the membranes (Fig. 14) after 2 h working in photocatalyst separation indicated that there was little difference to PAN700 membrane before and after experiment. But for PVDF700 membrane, it was very different. An obvious change occurred at the surface of membrane. In this case, we found the skin layer became more finely microporous and the former hole tended to be larger. The interface was coarser after TiO_2 rejection. Compared with common ultrafiltration process, this phenomena was very interesting and could be attributed to the property of, which predicted that the hydrophobic PVDF membrane was more easily hydrophilized by TiO_2 than originally hydrophilic PAN membrane. More research should be taken to elucidate this phenomena.

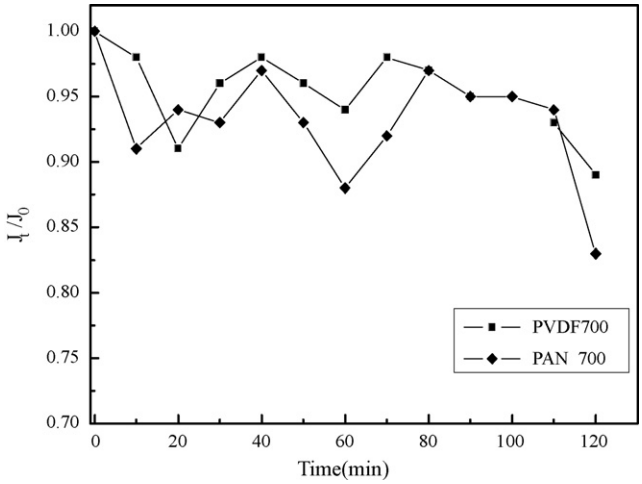

Fig. 11. Coupling photocatalysis with membrane separation.

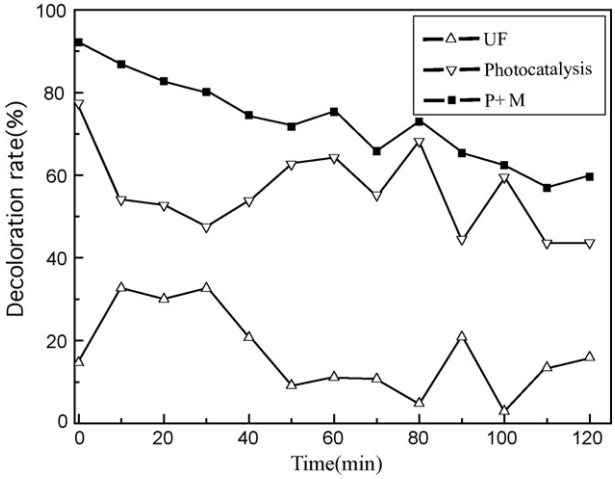

Fig. 13. Contribution of different parts in photocatalytic membrane reactor.

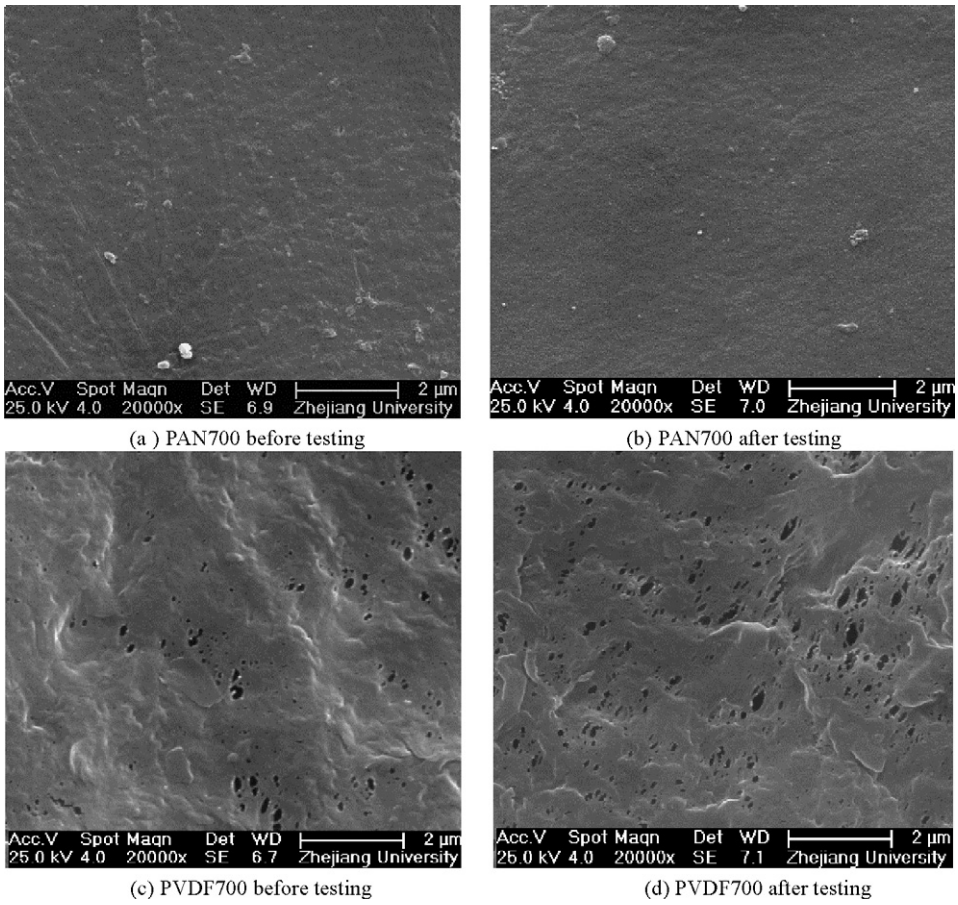

Fig. 14. SEM of membranes in the separation. (a) PAN700 before testing; (b) PAN700 after testing; (c) PVDF700 before testing and (d) PVDF700 after testing.

4. Conclusions

The reactor coupling the photocatalytic and ultrafiltration can successfully degrade the azo dye wastewater containing acid red B normally in the textile effluent. During the adsorption process, acid solution was propitious to the acid red B adsorption on the surface of TiO_2. The initial reaction rate (r_0) indicated that the optimal concentrations of TiO_2 and acid red B were 1.5 and 50 mg/L, respectively. After 120 min illumination by low pressure UV lamp, most of acid red B was mineralized. Single UF membrane separation process could remove some of the dye owing to the membrane retention and adsorption, but the drawback of large permeate flux decline was essential and could not be neglected, while in the coupling system it could be improved due to the conglomeration and hydrophilizion phenomena by TiO_2. Therefore, the photocatalytic membrane reactor was not only very effective to decompose the acid red B, but also take advantage of keeping permeate flux constant, which predicted potential application in the near future.

Acknowledgements

The authors thank Dr. J.X. Mo for useful discussion in the reactor design. This work was primarily funded by the Research Fund of the National Natural Science Foundation of China (grants 20476096 and 20776133). Other financial support came from the Research Fund from Zhejiang Provincial Bureau of Science and Technology (2006C23067) and Zhejiang Bureau of Education (Key Discipline of Environmental Engineering grants 56310503014).

References

[1] K. Sahel, N. Perol, H. Chermette, et al., Photocatalytic decolorization of Remazol Black 5 (RB5) and Procion Red MX-5B—isotherm of adsorption, kinetic of decolorization and mineralization, Appl. Catal. B: Environ. 77 (2007) 100–109.
[2] C.M. Zhu, L.Y. Wang, L.R. Kong, Photocatalytic degradation of AZO dyes by supported TiO_2 + UV in aqueous solution, Chemosphere 41 (2000) 303–309.
[3] T. Sauer, G.C. Neto, H.J. Jose, Kinetics of photocatalytic degradation of reactive dyes in a TiO_2 slurry reactor, J. Photochem. Photobiol. A: Chem. 149 (2002) 147–154.
[4] S. Mozia, et al., Effect of process parameters on photodegradation of Acid Yellow 36 in a hybrid photocatalysis–membrane distillation system, Chem. Eng. J. (2009), doi:10.1016/j.cej.2008.12.012.
[5] N. Guettai, H. Ait Amar, Photocatalytic oxidation of methyl orange in presence of titanium dioxide in aqueous suspension. Part II. Kinetics study, Desalination 185 (2005) 439–448.
[6] B. Bayarri, J. Gimenez, D. Curo, S. Esplugas, Photocatalytic degradation of 2,4-dichlorophenol by TiO_2/UV: kinetics, actinometries and models, Catal. Today 101 (2005) 227–236.
[7] M. Behnajady, N. Modirshahla, N. Daneshvar, Photocatalytic degradation of an azo dye in a tubular continuous-flow photoreactor with immobilized TiO_2 on glass plates, Chem. Eng. J. 127 (2007) 167–176.
[8] R. Molinari, C. Grande, E. Drioli, Photocatalytic membrane reactors for degradation of organic pollutants in water, Catal. Today 67 (2001) 273–279.
[9] J.F. Fu, M. Ji, Y.Q. Zhao, L.Z. Wang, Kinetics of aqueous photocatalytic oxidation of fulvic acids in a photocatalysis–ultrafiltration reactor (PUR), Sep. Purif. Technol. 50 (2006) 107–113.
[10] M.F.J. Dijkstra, E.C.B. Koerts, A.A.C.M. Beenackers, J.A. Wesselingh, Performance of immobilized photocatalytic reactors in continuous mode, AIChE. J. 49 (2003) 734–744.
[11] K. Azrague, P. Aimar, F. Benoit-Marquie, M.T. Maurette, A new combination of a membrane and a photocatalytic reactor for the depollution of turbid water, Appl. Catal. B: Environ. 72 (2007) 197–204.
[12] S.S. Chin, T.M. Lim, K. Chiang, A.G. Fane, Factors affecting the performance of a low-pressure submerged membrane photocatalytic reactor, Chem. Eng. J. 130 (2007) 53–63.
[13] F. Bosc, A. Ayral, C. Guizard, Mesoporous anatase coatings for coupling membrane separation and photocatalyzed reactions, J. Membr. Sci. 265 (2005) 13–19.

[14] H. Zhang, J. Chen, G. Zhang, Z. Yang, L. Ni, Organic dyeing wastewater treatment with photocatalysis and membrane separation hybrid system, in: IWA Regional Conference on Membrane Technologies in Water and Waste Water Treatment, Moscow, Russia, June 2–4, 2008.
[15] P. Le-Clech, E.K. Lee, V. Chen, Hybrid photocatalysis membrane treatment for surface waters containing low concentrations of natural organic matters, Water Res. 40 (2006) 323–330.
[16] N.M. Mahmoodi, M. Arami, Bulk phase degradation of Acid Red 14 by nanophotocatalysis using immobilized titanium (IV) oxide nanoparticles, J. Photochem. Photobiol. A: Chem. 182 (2006) 60–66.
[17] Z.G. Zhao, Principle of Adsorption Application, Chemical Industry Press, Beijing, 2005.
[18] K.H. Choo, D.I. Chang, K.W. Park, M.H. Kim, Use of an integrated photocatalysis/hollow fiber microfiltration system for the removal of trichloroethylene in water, J. Hazard. Mater. 152 (2008) 183–190.
[19] W.M. Xi, S. Geissen, Separation of titanium dioxide from photocatalytically treated water by cross-flow microfiltration, Water Res. 35 (2001) 1256–1262.